

The $H\alpha$ Luminosity Function and Global Star Formation Rate From Redshifts of One to Two

Lin Yan¹, Patrick J. McCarthy¹,

Wolfram Freudling², Harry I. Teplitz^{3,4}, Eliot M. Malumuth^{3,6},

Ray J. Weymann¹, Matthew A. Malkan⁵

ABSTRACT

We present a luminosity function for $H\alpha$ emission from galaxies at redshifts between 0.7 and 1.9 based on slitless spectroscopy with NICMOS on HST. The luminosity function is well fit by a Schechter function over the range $6 \times 10^{41} < L(H\alpha) < 2 \times 10^{43}$ erg sec⁻¹ with $L^* = 7 \times 10^{42}$ erg sec⁻¹ and $\phi^* = 1.7 \times 10^{-3}$ Mpc⁻³ for $H_0 = 50$ km s⁻¹ Mpc⁻¹ and $q_0 = 0.5$. We derive a volume averaged star formation rate at $z = 1.3 \pm 0.5$ of $0.13 M_\odot \text{ yr}^{-1} \text{ Mpc}^{-3}$ without correction for extinction. The SFR that we derive at $\sim 6500 \text{ \AA}$ is a factor of 3 higher than that deduced from 2800 \AA continua. If this difference is due entirely to reddening, the extinction correction at 2800 \AA is quite significant. The precise magnitude of the total extinction correction at rest-frame UV wavelengths (e.g. 2800 \AA and 1500 \AA) is sensitive to the relative spatial distribution of the stars, gas and dust, as well as on the extinction law. In the extreme case of a homogeneous foreground dust screen and a MW or LMC extinction law, we derive a total extinction at 2800 \AA of 2.1 magnitudes, or a factor of 7 correction to the UV luminosity density. If we use the Calzetti reddening curve, which was derived for the model where stars, gas and dust are well mixed and nebular gas suffers more extinction than stars, our estimate of A_{2800} is increased by more than one magnitude.

Subject headings: Galaxies: emission lines, luminosity function, evolution

¹The Observatories of the Carnegie Institution of Washington,
813 Santa Barbara St., Pasadena, CA 91101

²Space Telescope European Coordinating Facility, Karl-Schwarzschild-Str. 2. D-85748
Garching bei Munchen, Germany

³NASA Goddard Space Flight Center, Code 681, Greenbelt, MD 20771

⁴NOAO Research Associate

⁵Astronomy Department, University of California, Los Angeles, CA 90024-1562

⁶Raytheon STX Corp., Lanham, MD 20706

1. Introduction

The global star formation history of the universe holds clues to understanding the formation and evolution of galaxies. The recent detections of dust enshrouded galaxies at $z > 1$ at sub-millimeter wavelengths (Smail, Ivison & Blain 1997; Hughes et al. 1998; Barger et al. 1998; Lilly et al. 1998) suggest that significant amounts of star formation activity at high redshifts may be obscured. UV-selected galaxies most likely represent only one segment of the population of active star-forming systems at early epochs. The difficulty in estimating the degree of extinction in the rest-frame UV introduces significant uncertainties in the star formation history (Pettini et al. 1998; Heckman et al. 1998; Blain et al. 1999; Malkan 1998).

Little is known about the properties of normal galaxies in the region between $1 < z < 2$, where neither the 4000Å break nor the Ly continuum break are easily accessible. The determinations of the global star formation history based on either the 2500Å and 1500Å continuum luminosities, or on the abundance of damped Ly α systems (e.g. Pei & Fall 1995; Madau et al 1996; Steidel et al. 1998, Pei, Fall, & Hauser 1999), imply either a peak or a plateau in the $1 < z < 2$ range. The near-IR offers one means of accessing both redshift indicators and measures of star formation at these redshifts.

NICMOS offered a unique opportunity to perform slitless spectroscopy in the near-IR. The extremely low background achieved on HST at $\lambda < 1.9\mu$ allows for sensitive surveys for H α to $z = 1.9$. We carried out a survey of random fields with the slitless G141 grism ($\lambda_c = 1.5\mu$, $\Delta\lambda = 0.8\mu$), covering a total ~ 64 square arc-minutes (McCarthy et al. 1999; hereafter paper I). Our survey has equal or greater depth than current ground-based narrow-band imaging programs, and due to its large wavelength coverage probes an order of magnitude more co-moving volume. The details of the survey and the spectra of the emission-line objects are given in paper I.

In this *Letter* we present the H α luminosity function at $0.7 < z < 1.9$ derived from the H α emission-line galaxy sample described in Paper I. We also discuss the implications of our results in the context of galaxy formation and evolution. Throughout this paper we use $H_0 = 50 \text{ km s}^{-1} \text{ Mpc}^{-1}$ and $q_0 = 0.5$.

2. The H α Luminosity Function at $z \sim 0.7 - 1.9$

2.1. The properties of the sample

The bandpass of the G141 grism in camera 3 of NICMOS limits the range of redshifts within which we can detect H α to $0.7 - 1.9$. The identification of the emission lines as H α is based on H-band apparent continuum magnitudes, their equivalent widths and the lack of other detected lines within the G141 bandpass. In two of the three cases for which optical spectroscopy has been attempted with LRIS on the Keck 10m telescope by Teplitz et al. (1999), the line identifications

have been confirmed by detection of their [OII]3727 emission. These objects (J0055+8518a, $z = 0.76$, J0622-0018a, $z = 1.12$) are at the low redshift end of our sample and therefore are the most accessible to optical spectroscopy. In the third case (J1237+6219A, $z = 1.37$) no emission or absorption features were detected in the spectrum.

2.2. Calculation of the H α luminosity function at $z \sim 0.7 - 1.9$

We used the $1/V_{\max}$ method (Schmidt 1968) to compute the luminosity function. Each galaxy is assigned a volume, V_{\max} , equal to the volume within which it could lie and be detected by our survey. We calculated the maximum co-moving volume for each galaxy in each field with its appropriate line flux limit. The maximum volume is defined as

$$V_{max} = \Omega \times \int_{zmin}^{zmax} \left(\frac{c}{H_0} \right)^3 \frac{1}{(1+z)^3} \frac{(q_0 z + (q_0 - 1)(\sqrt{1 + 2q_0 z} - 1))}{q_0^4 \sqrt{1 + 2q_0 z}} dz, \quad (1)$$

where $zmin$ and $zmax$ are the minimum and maximum redshifts. $zmin = 0.67$, the lower spectral cutoff of the NICMOS G141 grism. The maximum redshift at which an object can be detected, $zmax$, is $\min(1.9, z2)$, where $z2$ is computed from $D_L(zmax) = D_L(z) \sqrt{\frac{f(H\alpha)}{f_{lim}}}$, and D_L is the luminosity distance at redshift z . $f(H\alpha)$ and f_{lim} are the H α line flux and the flux limit, respectively. Ω is the solid angle subtended by a single NICMOS camera 3 image. Only the central portion of each grism image samples the full range of wavelengths from $1.1\mu - 1.9\mu$, and the left and right portions of the image sample restricted spectral ranges. The field of view subtended by the central section is $\sim 31'' \times 49''$; the two sides of the image subtend roughly $10'' \times 49''$ each. Thus the volume must be calculated separately for each portion of the detector. The grism sensitivity is a function of wavelength and this influences the effective volume probed, particularly at the ends of the spectral coverage, where the sensitivity (and hence the available volume) fall off steeply.

The estimate of the source density in a luminosity bin of width $\Delta(\log L)$ centered on luminosity $\log L_i$ is simply the sum of the inverse volumes ($1/V_{\max}$) of all the sources with luminosities in the bin. The value of the luminosity function in that bin is

$$\phi(\log L_i) = \frac{1}{\Delta(\log L)} \sum_{|\log L_j - \log L_i| < \Delta(\log L)} \frac{1}{V_{max,j}} \quad (2)$$

where index i labels luminosity bins and index j labels galaxies. The variances are computed by summing the squares of the inverse volumes; the error bars of each luminosity bin are the square roots of the variances.

The apparent luminosity function must be corrected for incompleteness in the original source catalog. The approach we adopted is similar to that used in Yan et al. (1998). We chose several

well-detected emission-line galaxies spanning a range of W_λ in the form of 2D spectra. We dimmed these template spectra by various factors and added them to the real NICMOS grism images at random locations. We then applied the same detection procedure as in the original analyses (see Paper I) to recover the template spectra. The use of random positions in the simulation allows us to include incompleteness corrections caused by crowding and spatially dependent errors in the sky subtraction and shading corrections. We added the dimmed template spectra to the 2D grism images with a wide range of sensitivities to simulate the true distribution of limiting fluxes in our survey fields. The final averaged detection rate provides a measurement of the dependence of the detection probability on the line flux limits, as well as equivalent width for $W_{rest} > 50\text{\AA}$. The incompleteness correction is applied to each bin independently.

In Figure 1 we show our derived luminosity function and the local $H\alpha$ LF as measured by Gallego et al. (1995). Our $H\alpha$ luminosities have been corrected for [NII] contamination using $H\alpha/[NII]6583,6548 = 2.3$ (Kennicutt 1992; Gallego et al. 1996). The solid and dashed lines are the best fits to a Schechter luminosity function at $z \sim 1.3$ and $z \sim 0$, respectively. Gallego et al. (1995) derived $L^*(H\alpha) = 1.4 \times 10^{42} \text{ erg s}^{-1}$, $\alpha = -1.35$ and $\phi = 6.3 \times 10^{-4} \text{ Mpc}^{-3}$. We obtain $L^*(H\alpha) = 7 \times 10^{42} \text{ erg s}^{-1}$ and $\phi = 1.7 \times 10^{-3} \text{ Mpc}^{-3}$, assuming a faint end slope, α , equal to the local value of -1.35 . Our sample is not large enough or deep enough to allow an independent determination of α .

Figure 1 shows strong evolution in the $H\alpha$ luminosity density from $z \sim 0$ to $z \sim 1.3$. This is no surprise given the evolution in the ultraviolet luminosity density, but our result provides an independent measure of evolution for $H\alpha$ emission alone. The integrated $H\alpha$ luminosity density at $z \sim 1.3$ (our median z) is $1.64 \times 10^{40} h_{50} \text{ erg s}^{-1} \text{ Mpc}^{-3}$, approximately 14 times greater than the local value reported by Gallego et al. (1995). Gronwall (1998) has reported a preliminary measure of the local star formation density derived from the KISS survey that is consistent with the Gallego et al. value. If the faint end slope is as steep as -1.6 , as found for the UV luminosity function at $z \sim 3$ (Steidel et al. 1999; Pascarelle, Lanzetta & Fernandez-Soto 1998), the integrated $H\alpha$ luminosity density at $z \sim 1.3$ would be roughly 50% higher still. Two of the emission-line galaxies in our sample are possible AGN candidates. If we remove the top three objects with the highest $H\alpha$ fluxes from our luminosity function calculation, the integrated $H\alpha$ luminosity density is reduced by $\sim 40\%$, primarily due to the decrease of $L^*(H\alpha)$.

3. Implications for the Evolution of Field Galaxies

We converted the integrated $H\alpha$ luminosity density to a star formation rate (SFR) using the relation from Kennicutt (1999): $\text{SFR}(M_\odot \text{ yr}^{-1}) = 7.9 \times 10^{-42} L(H\alpha) (\text{erg s}^{-1})$. This assumes Case B recombination at $T_e = 10^4 \text{ K}$ and a Salpeter IMF ($0.1 - 100 M_\odot$). This conversion factor is about 10% smaller than the value listed in Kennicutt (1983), the difference reflecting updated evolutionary tracks. While different choices of stellar tracks introduce modest uncertainties in the conversion of UV and $H\alpha$ luminosities to star formation rates, the choice of different IMFs

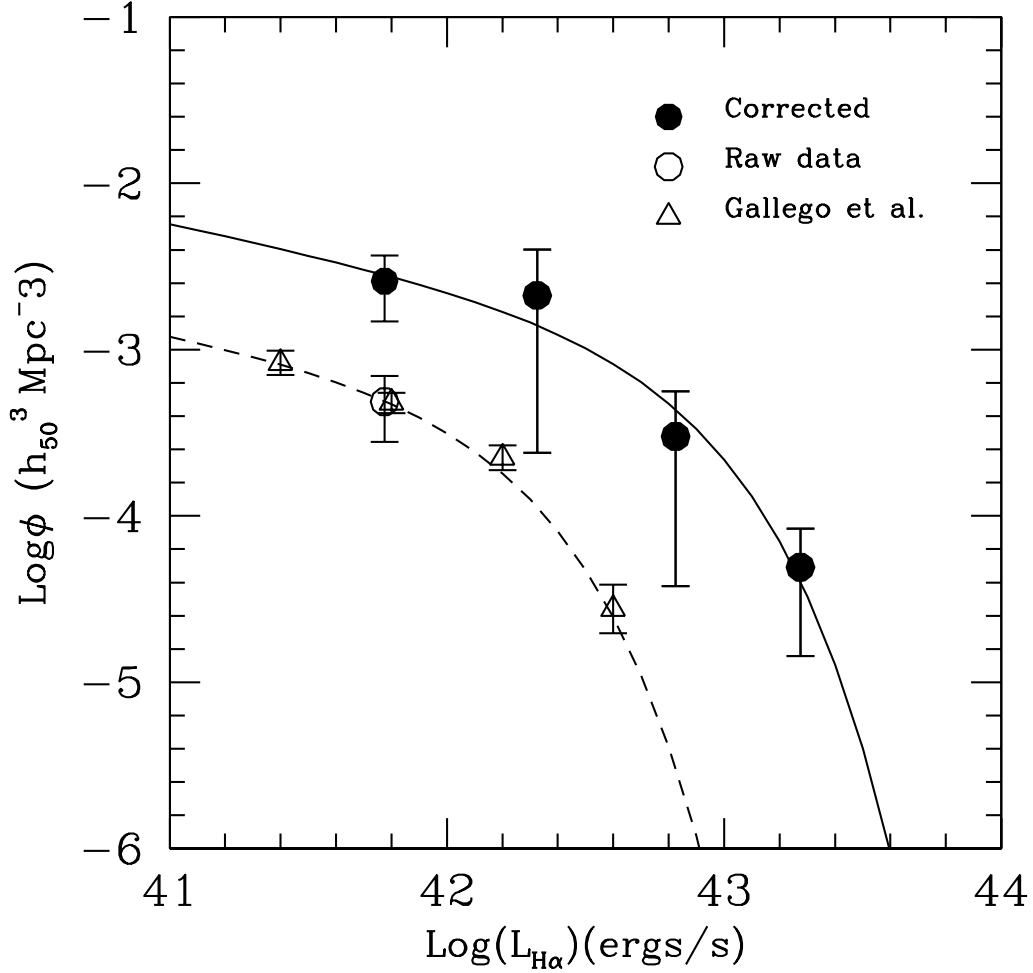


Fig. 1.— $\text{H}\alpha$ luminosity function at $0.7 < z < 1.9$. The open and filled circles are the data points from our measurements. The open circles represent the raw data and the filled circles are the points corrected for incompleteness. The incompleteness correction is only significant at the faintest luminosity bin. The open triangles show the local $\text{H}\alpha$ luminosity function by Gallego et al. (1995). The solid and dashed lines are the best fits to the data at $z \sim 1.3$ and $z \sim 0$ respectively.

lead to rather large differences. To make consistent comparisons between our results and those in the literature derived from 1500Å and 2800Å UV continuum luminosity densities, we adopt the relation from Kennicutt (1999): $\text{SFR}(M_{\odot}\text{yr}^{-1}) = 1.4 \times 10^{-28} L(1500 - 2800\text{Å})(\text{erg s}^{-1}\text{Hz}^{-1})$. This relation is appropriate for the Salpeter IMF used to derive the H α conversion factor.

In Figure 2, we plot uncorrected published measurements of the volume-averaged global star formation rate at various epochs. The open squares represent measurements of the 2800Å or 1500Å continuum luminosity density by Lilly et al. (1996), Connolly et al. (1996) and Steidel et al. (1998); the filled squares are the measurements using H α 6563Å by Gallego et al. (1995), Tresse & Maddox (1996) and Glazebrook et al. (1998). Our result is shown as a filled circle. The star formation rates shown in Figure 2 are calculated from the luminosity densities integrated over the entire luminosity functions, for both H α and the UV continuum. Lilly et al. and Connolly et al. assumed a faint end slope of -1.3 for the UV continuum luminosity functions at $z \leq 1$. The 1500Å continuum luminosity function at $z \sim 3 - 4$ measured from Lyman break galaxies by Steidel et al. (1998) has a faint end slope of -1.6 .

Glazebrook et al. (1998) measured H α line fluxes for 13 CFRS galaxies at $z \sim 1$ and concluded that the star formation rate deduced from H α is significantly larger than that derived from the 2800Å continuum luminosity density. Using the conversion factors which we have employed throughout this paper (7.9×10^{-41} for H α and 1.4×10^{-28} for the UV continuum), we estimate that without correcting for extinction the star formation rate derived from their H α luminosity density is a factor of 1.9 higher than that inferred from the 2800Å continuum. The factor of 3 difference in the star formation rate between H α and the UV continuum noted in Glazebrook et al. (1998) includes an extinction correction. As discussed below, the magnitude of the extinction correction is highly dependent on the relative spatial distributions of stars, gas and dust.

Pettini et al. (1998) found the star formation rates of Lyman break galaxies at $z \sim 3$ measured from H β emission to be $0.7 - 7\times$ higher than those estimated from the 1500Å continuum. Hogg et al. (1998) and Hammer et al. (1997) derived the [OII]3727 luminosity function and detected strong evolution in the [OII] luminosity density to $z = 1.3$. The conversion factor from the [OII]3727 luminosity to a SFR, however, can differ by an order of magnitude, depending on the metallicity of the gas (Gallagher, Hunter & Bushouse 1989; Kennicutt 1992). In contrast, H α provides a more direct measure of the star formation by effectively reprocessing the integrated stellar luminosity of galaxies shortward of the Lyman limit. Recent observations at sub-mm wavelengths indicate the star formation rate at $2 < z < 4$ is larger than that inferred from the rest-frame UV luminosity density (Hugh et al. 1998). The contribution of the sub-mm sources to the global star formation history is uncertain at this time, as most of the sub-mm sources do not have secure redshifts (Barger et al. 1999).

The clear trend for the longer wavelength determinations of the star formation rate to exceed those based on UV continua is one of the pieces of evidence for significant extinction at intermediate and high redshifts. The amplitude of the extinction correction is quite uncertain

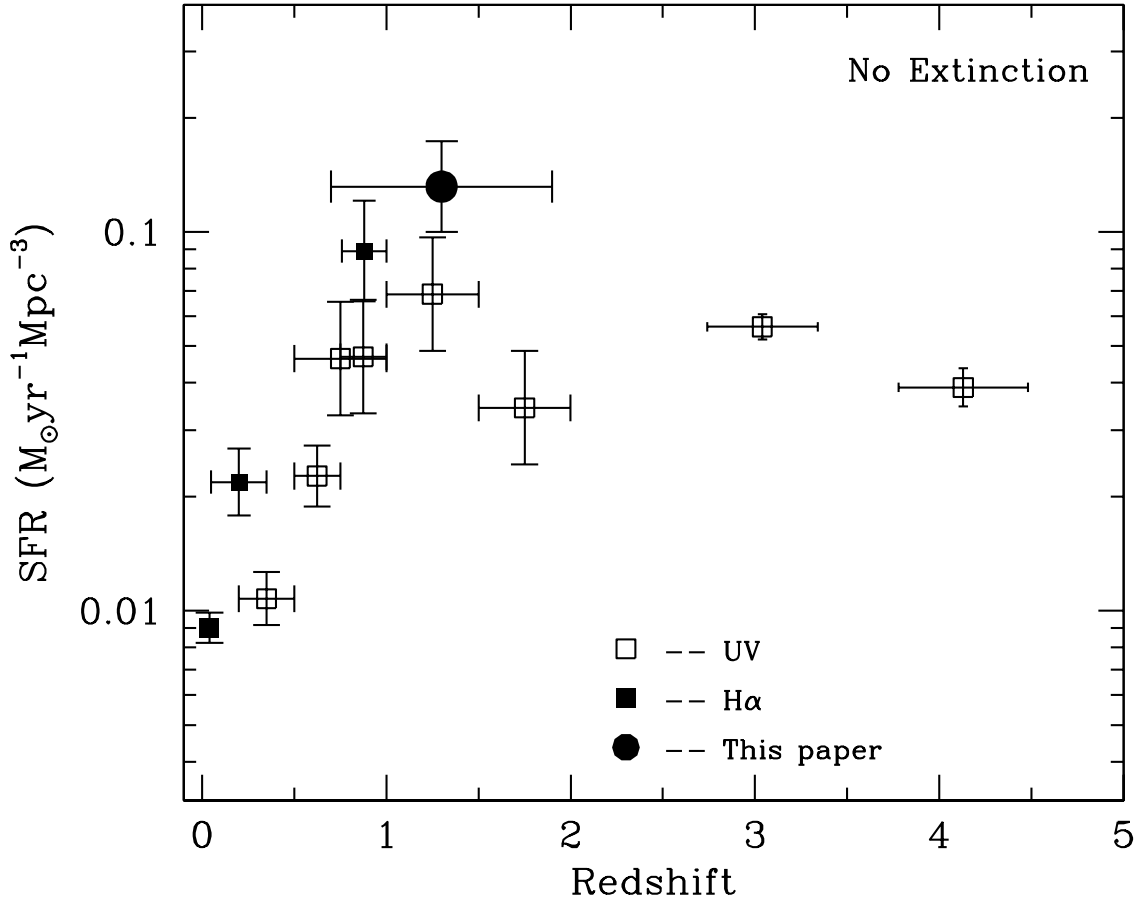


Fig. 2.— The global volume-averaged star formation rate as a function of redshift without any dust extinction correction. The open squares represent measurements of the 2800Å or 1500Å continuum luminosity density by Lilly et al. (1996), Connolly et al. (1996) and Steidel et al. (1998), whereas the filled squares are the measurements using H α 6563Å by Gallego et al. (1995), Tresse & Maddox (1996) and Glazebrook et al. (1998). Our result is shown in the filled circle.

(e.g. Heckman et al. 1997; Meuers et al. 1997; Steidel et al. 1998). Our measurement spans $0.7 < z < 1.9$, overlapping with the Connolly et al. photometric redshift sample and allowing a direct comparison between the observed 2800\AA luminosity density and that inferred from $\text{H}\alpha$. The emission line galaxies selected by our survey have a co-moving number density similar to that of the bright Lyman break galaxies at $z \sim 3$, and a median H magnitude that corresponds to approximately L^* (Paper I). While we are not comparing the same individual galaxies, the rough correspondence in space density and continuum absolute magnitudes between the UV- and $\text{H}\alpha$ -selected samples argues that they are drawn from similar or overlapping populations. Our $\text{H}\alpha$ -based star formation rate is three times larger than the average of the three redshift bins measured by Connolly et al. (1997).

The star formation rates derived from line or continuum luminosities depend strongly on the choice of IMF, evolutionary tracks, and stellar atmospheres that are input into a specific spectral evolution model. The relevant issue for the present discussion is the ratio of the star formation rates derived from $\text{H}\alpha$ and the 2800\AA continuum. As shown by Glazebrook et al. (1998) this ratio differs significantly for the Scalo and Salpeter IMFs and is a function of metallicity. Our choice of the Salpeter IMF comes close to minimizing the difference between the published UV- and our $\text{H}\alpha$ -derived star formation rates. The use of a Scalo IMF and solar metallicity would increase the apparent discrepancy by a factor of ~ 2 . The only model considered by Glazebrook et al. that further reduces the $\text{H}\alpha/2800\text{\AA}$ star formation ratio is the Salpeter IMF with the Gunn & Stryker (1983) spectral energy distributions, and this model still leaves us with a factor of ~ 2 enhancement in apparent star formation activity measured at $\text{H}\alpha$.

If we attribute the entire difference to reddening, the total extinction corrections at 2800\AA and $\text{H}\alpha$ are large and model-dependent. The calculation is sensitive to the relative geometry of the stars, gas and dust, as well as the adopted reddening curve. In the extreme case of a homogeneous foreground screen and a MW or LMC reddening curve, we derive $A_{2800} = 2.1$ magnitudes. In local starburst galaxies, differential extinction between the nebular gas, and stellar continuum, and scattering produce an effective reddening curve that is significantly grayer than the MW or LMC curves (Calzetti, Kinney & Storchi-Bergmann 1994; 1996; Calzetti 1997). The Calzetti reddening law (Calzetti 1997) is appropriate for geometries in which the stars, gas and dust are well mixed. In this model, our estimate of the dust extinction at 2800\AA is one to two magnitudes larger than in the simple screen case, and is an uncomfortably large correction compared to results from other methods (e.g., Heckman et al. 1998; Steidel et al. 1999).

The properties of the damped $\text{Ly}\alpha$ absorbers, diffuse backgrounds and galaxy counts at long wavelengths provide independent constraints on the amount of obscured star formation at large redshifts (e.g. Pei, Fall, & Hauser 1999; Calzetti & Heckman 1998; Blain et al. 1999). Our measurement of the global star formation rate derived from $\text{H}\alpha$ agrees well with the model predictions in Figure 7 of Pei, Fall, & Hauser.

Despite our efforts to quantify the incompleteness of the NICMOS grism sample, some biases

remain. The low resolution of the grisms prevent efficient detection of objects with line fluxes above our threshold but with rest-frame $W_{rest} < 50\text{\AA}$. The Gallego et al. (1995) survey has a W_λ threshold of 10\AA . Gallego et al. (1996) find that dwarf amorphous nuclear starbursts have modest equivalent widths but contribute little to the total luminosity density. Some of the compact starburst nuclei will fall below our W_λ threshold, and these objects can have substantial luminosities. Their compact size mitigates against this somewhat as our spectral resolution is best for point sources. $H\alpha$ spectroscopy of galaxies from the CFRS sample at $z < 0.3$ by Tresse & Maddox (1996) weakly suggests that $W_\lambda(H\alpha)$ and luminosity are correlated.

HST imaging and spectroscopic samples all suffer from a bias against low surface brightness objects. The slitless nature of our survey exacerbates the problem as the spectral resolution is a function of apparent source size. The half-light radii of the emission line galaxies in our sample range from $0.2''$ to $0.7''$ and the distribution is comparable to that seen in significantly deeper fields, such as the HDF-South and deep NICMOS parallel fields (Yan et al. 1998; Storrie-Lombardi et al. 1999).

The principal conclusions of this work are that the $H\alpha$ luminosity density at $z = 1.3$ is an order of magnitude larger than locally, that the global star formation rate derived from our $H\alpha$ measurements exceeds that from the rest-frame UV by a factor of 3 and the implied extinction corrections are substantial. Although the characteristics of this particular data set do not lend themselves to precise comparison between global averaged star formation rates inferred from UV continuum and line-emission, the systematically larger rates inferred from $H\alpha$ at all redshifts point towards significant extinction at rest-frame UV wavelengths.

4. Acknowledgments

We thank the staff of the Space Telescope Science Institute for their efforts in making this parallel program possible. In particular we thank John Mackenty, Duccio Machedto, Peg Stanley, Doug van Orsow, and the staff of the PRESTO division. We acknowledge useful discussions with M. Fall, J. Gallego, D. Calzetti and R. Marzke. This research was supported, in part, by grants from the Space Telescope Science Institute, GO-7499.01-96A, AR-07972.01-96A and PO423101. HIT acknowledges funding by the Space Telescope Imaging Spectrograph Instrument Definition Team through the National Optical Astronomy Observatories and by the NASA Goddard Space Flight Center.

REFERENCES

- Barger, A.J., Cowie, L.L., Sanders, D.B., Fulton, E., Taniguchi, Y., Sato, Y., Kawara, K., Okuda, H., 1998, *Nature*, 394, 248
- Blain, A.W., Smail, I., Ivison, R.J. & Kneib, J.-P., 1999, *MNRAS*, 302, 632
- Calzetti, D. 1997, *AJ*, 113, 162

- Calzetti, D. & Heckman, T. 1999, ApJ, in press. astro-ph/9811099
- Calzetti, D., Kinney, A.L. & Storchi-Bergmann, T. 1994, ApJ, 429, 582
- Calzetti, D., Kinney, A.L. & Storchi-Bergmann, T. 1996, ApJ, 458, 132
- Connolly, A., Szalay, A. S., Dickinson, M., Subbarao, M., Brunner, R. J. 1997, ApJ, 487, L13
- Gallego, J., Zamorano, J., Rego, M., Alonso, O. & Vitores, A.G. 1996, A&AS, 120, 323
- Gallego, J., Zamorano, J., Aragon-Salamanca, A., Rego, M. 1995, ApJL, 459, 1
- Glazebrook, K., Blake, C., Economou, F., Lilly, S. & Colless, M. 1998, astro-ph/9808276
- Gronwall, C. 1998, in "Dwarf Galaxies and Cosmology", eds. T. Thuan et al., Editions Frontieres, in press. astro-ph/9806240
- Hammer, F., Flores, H., Lilly, S.J., Crampton, D., Le Fevre, O., Rola, C., Mallen-Ornelas, G., Schade, D. & Tresse, L. 1997, ApJ, 481, 49
- Heckman, T., Robert, C., Leitherer, C., Garnett, D.R., van der Rydt, F. 1998, ApJ, 503, 646
- Hogg, D., Cohen, J. G., Blandford, R., Pahre, M. 1998, ApJ, 504, 622
- Hughes, D., et al. 1998, Nature, 394, 241.
- Kennicutt, R.C. 1983, ApJ, 272, 54
- Kennicutt, R.C. 1992, ApJ, 388, 310
- Kennicutt, R.C. 1999, ARAA, in press. astro-ph/9807187
- Lilly, S.J., Le Fevre, O., Hammer, F. & Crampton, D. 1996, ApJ, 460, L1
- Lilly, S.J., Eales, S.A., Gear, W.K.P., Hammer, F., Le Fevre, O., Crampton, D., Bond, J.R., Dunne, L., 1999, ApJ, in press. astro-ph/9901047
- Madau, P., Ferguson, H., Dickinson, M., Giavalisco, M., Steidel, C., & Fruchter, A. 1996, MNRAS, 283, 1388
- Madau, P., Pozzetti, L. & Dickinson, M. 1998, ApJ, 498, 106
- Malkan, M. 1998, astro-ph/9810055
- McCarthy, P., Yan, L., Freudling, W., Teplitz, H. I., Eliot M. Malumut, E. M., Weymann, R. J., Malkan, M. A., Fosbury, R. A. E., Gardner, J. P., Storrie-Lombardi, L., Thompson, R. I., Williams, R. E., Heap, S. R. 1999, ApJ, in press. astro-ph/9902347
- Meurer, G.R., Heckman, T.M., Lehnert, M.D., Leitherer, C. & Lowenthal, J. 1997, AJ, 114, 54

- Pascarelle, S.M., Lanzetta, K.M. & Fernandez-Soto, A. 1998, ApJ, 508, 1L
- Pei, Y.C. & Fall, S.M. 1995, ApJ, 454, 69
- Pei, Y.C., Fall, S.M., Hauser, M. 1999, ApJ, in press. astro-ph/9812182
- Pettini, M., Kellogg, M., Steidel, C.C., Dickinson, M., Adelberger, K.L., Giavalisco, M. 1998, ApJ, 508, 539
- Smail, I., Ivison, R.J. & Blain, A.W. 1997, ApJ, 490, L5
- Schmidt, M. 1968, ApJ, 151, 393
- Steidel C., Dickinson, M., Giavalisco, M. Pettini, M., Adelberger, K. 1998, ApJ, in press. astro-ph/9811399
- Storrie-Lombardi, L., Weymann, R. J., Thomspon R. et al. 1999, in preperation.
- Teplitz, H., Malkan, M. A., McLean, I. S. 1998, ApJ, 506, 519
- Teplitz, H., Malkan, M. A., McLean, I. S. 1999, ApJ, in press
- Teplitz, H., Malkan, M. et al. 1999, in prep.
- Tresse, L., Maddox, S. 1998, ApJ, 495, 691
- van der Werf, P.P., Bremer, M. N., Moorwood, A. F. M., Rottgering, H. J. A. 1997, IAU, 186, 197
- Yan, L., McCarthy, P.J., Storrie-Lombardi, L.J., Weymann, R.J., 1998, ApJ, 507, L19